Macromolecules

ARTICLE

pubs.acs.org/Macromolecules

Stem Tilt in the Contact Plane of Epitaxially Grown Polylactide Lamellae and Its Direct Correlation with Lamellar Bending

Feng-Der Wang,[†] Jrjeng Ruan,*[,†] Yi-Fang Huang,[†] and An-Chung Su[‡]

[†]Department of Materials Science and Engineering, National Cheng Kung University, Tainan 701, Taiwan

[‡]Department of Chemical Engineering, National Tsing Hua University, Hsinchu 300, Taiwan

ABSTRACT: Via transmission electron microscopy, it was revealed that epitaxial crystallization on hexamethylbenzene substrate led to oriented arrays of individual long-chain poly(L-lactide) edge-on lamellae. Selected-area electron diffraction patterns indicated orientational deviations of packed stems from lamellar normal, i.e., stem tilt on the *bc* contact plane as a result of stairlike stem packing. Upon growth beyond edges of underneath substrates, correlated bending of lamellae in a counterclockwise manner was developed. The direct relationship between the tilted stem orientation and the bending sense of lamellar growth supports the notion of more severe accumulation of fold surface stresses around acute corners of growth fronts created by the stairlike packing scheme. Selected molecular weights and growth temperatures caused the changes in the magnitude of stem tilt, further manifesting the role of fold-loop repulsion on lamellar basal planes in creating surface stresses. In contrast, the type of chiral center on polylactide backbone appears to have played an important role in tilted orientation of stem packing during lamellar growth.

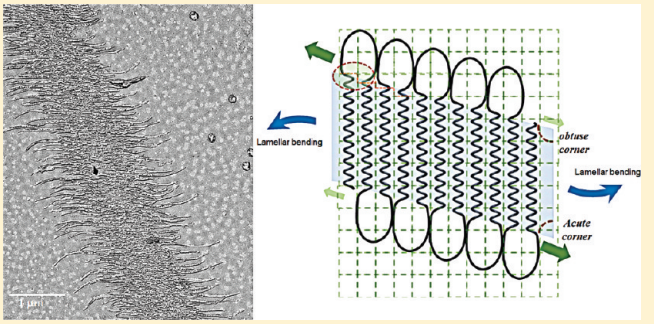

INTRODUCTION

Polymers with flexible backbone frequently adopt folded conformation for efficiently participating crystal growth. This habit requires parts of molecular chains to stay in a noncrystalline state during crystallization, as being included in fold loops and residual segments. Upon establishing lattice packing of transverse molecular stems, these noncrystalline molecular segments are restricted around interfaces. While sufficient space is not available on lamellar basal planes, surface stresses can be accumulated due to mutual repulsion and increase via continuously adding molecular stems into lattice packing. This can result in (either regular or random) staggered schemes of fold loops/packed molecular stems, which creates more space and lessens the crowdedness on basal planes.[1−4] Being attributed to sequential staggers involved during stem packing, a nonparallel relationship between stem orientation and lamellar normal (tilted stem packing) has been identified, as being found in the cases of hollow-pyramid single crystals of polyethylene (PE) and polyoxymethylene.[5−9]

In addition to stem tilt, an uneven distribution of interfacial stresses has been intensely discussed as one of the major causes of lamellar twisting or bending.[10−13] Nevertheless, the occurrences of nonplanar lamellar growth have been addressed either with or without the involvement of tilted stem packing.[14,15] The connection between stem tilt and nonplanar lamellar morphology thus remains an interesting issue to be further clarified.[11]

Presumably reflecting the interfacial crowdedness,[2,16] the degree of stem tilt is expected to vary with the factors capable of influencing lamellar basal phases, including growth temperature, diluent concentration, mixing with other polymers, and folding mechanism of either adjacent-reentry or switchboard fold models.[17−19] Experimentally, the angle of stem tilt has been found to vary from 19° to 41° for PE lamellae grown under various crystallization conditions.[20−22] In spite of providing better interfacial accommodation of fold loops, tilted stem packing also results in partial loss of lattice interactions between neighboring stems near folding surfaces. Thus, a compromise between these two opposing mechanisms has to be reached, which also adjusts the interfacial free energy and thus crystal stability.[3,23] It has been observed that disparate degrees of stem tilt in different sectors of PE truncated lozenges are present, and thus there are two levels of metastability (in terms of melting temperature, T_m) and lamellar thickness found within one single crystal.[24]

Reported here are our recent observations on individual growth of crystalline lamellae into oriented arrays via epitaxial crystallization of polylactides on crystalline hexamethylbenzene (HMB) substrates. Selected-area electron diffraction patterns (SAED) indicated orientational deviations of packed stems from the lamellar normal on the *bc* contact plane. This corresponds to stem tilting on a plane orthogonal to the conventionally acknowledged (*ac*) plane of stem tilting found in flat-on lamellae. The

Received: March 4, 2011
Revised: April 26, 2011
Published: May 13, 2011

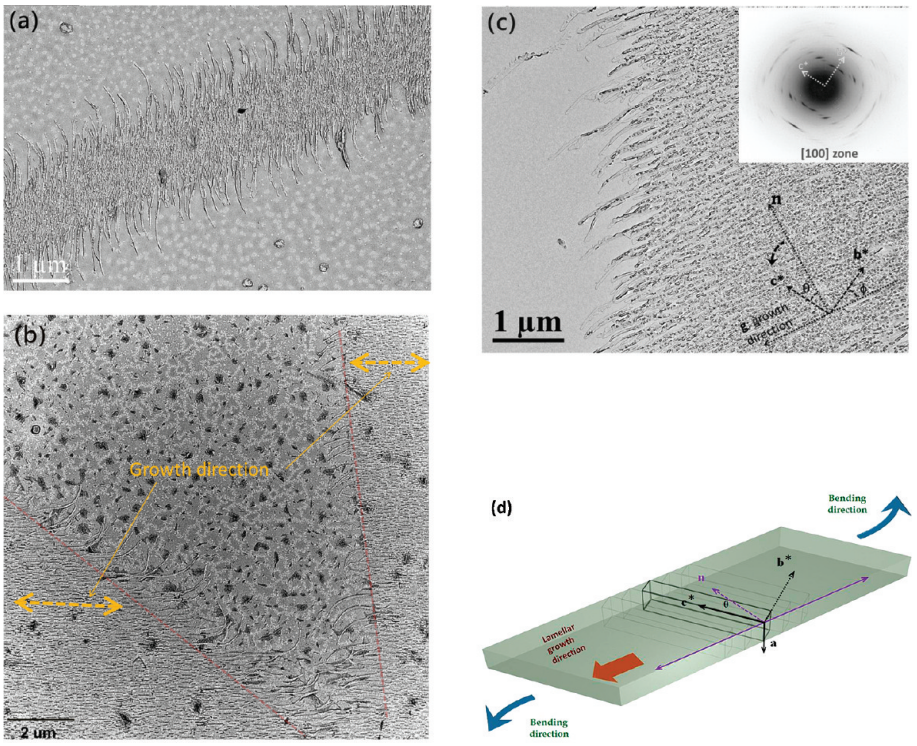

Figure 1. (a) Representative BFI of HMW-PLLA crystalline lamellae epitaxially grown at T_c = 150 °C on HMB crystalline substrate, illustrating oriented array of individual *edge-on* lamellae with correlated CCW bending pattern at both ends of lamellar growth. (b) A selected BFI spanning two independent arrays of HMW-PLLA lamellae, illustrating that there is no orientational relationship between the substrate edges and lamellar growth directions. The main parts of lamellar growth remain straight; the bending pattern is able to develop only near the ends of lamellar growth. The substrate boundaries are indicated by red dashed lines. (c) The inset is the [100] zone SAED pattern of the orthorhombic phase obtained from a larger area of lamellar array. After verifying the SAED orientation relative to corresponding arrayed edge-on lamellae, the c^*-direction of molecular stems was realized to deviate from lamellar normal direction, denoted as **n**, where θ signifies the CCW deviation angle. (d) Schematic representation of tilted lattice packing (represented by gray line) in the *bc* contact plane. The molecular stems are oriented along the c^*-axis, which deviates from the lamellar normal; the lamellar growth direction also deviates from the b^*-axis of the orthorhombic lattice.

extent of stem tilting depends on crystallization temperature (T_c) and chain length, and in contrast, the type of chiral center on polylactide backbones was found to correlate with bending senses of lamellae upon growth beyond substrates (and hence the loss of epitaxial contact). The latter observation signifies the role of stem tilting in lamellar bending in terms of disparity in accumulated surface stresses around lamellar corners on growth fronts.

EXPERIMENTAL SECTION

Materials/Sample Preparation. Long-chain poly(L-lactide) and poly(D-lactide) samples with nominal molecular masses of 40−60 kDa (HMW-PLLA) and 90 kDa (HMW-PDLA), respectively, were purchased from Sigma-Aldrich and used without further purification. Shorter chain molecules, including PLLA samples named LMW-PLLA of 9 kDa molecular masses with polydispersity index close to 1.2 and 20 kDa PDLA samples named LMW-PDLA, were synthesized using benzyl alcohol/tin octanoate in a sealed flask at 110 °C. The selected nucleation agent is hexamethylbenzene (HMB, T_m = 166 °C), which is of commercial origin (Sigma-Aldrich) and used without further purification also.

The sample preparation generally started with drop casting of dilute polylactide/*p*-xylene solutions into thin films typically 10−50 nm in thickness on glass cover slides. A small amount of HMB in triclinic form[25] was deposited on a separate glass slide and then brought to contact with the previously prepared polylactide film by flipping the glass slide. The sandwich was left on a hot surface (∼175 °C) to allow for partial mixing of HMB and polylactide. The sandwiched sample was then transferred to the crystallization temperature T_c = 150 or 132 °C. After cooling, the glass slides were separated, allowing for the removal of HMB via sublimation. The exposed polymer film was then backed with carbon, and the PLLA/carbon film was detached from the glass slide using a poly(acrylic acid) adhesive. The prepared film was then flipped over, left floating on water surface to wash away the adhesive, and then picked up using support grids for observations with transmission electron microscopy (TEM).

Transmission Electron Microscopy. Observations were made by use of a JEOL JEM-1400 instrument operated at 120 kV; bright-field images (BFI) were obtained using a Gatan digital detector, whereas selected-area electron diffraction (SAED) patterns were recorded on photographic films.

RESULTS

Relationship between Stem Tilting and Lamellar Bending. Figure 1a shows the prevailing growth of oriented arrays of individual edge-on lamellae of HMW-PLLA on crystalline surface of selected nucleation agent HMB at T_c = 150 °C. The oriented growth of individual lamellae manifests the influence of lattice interaction with the crystalline HMB substrate. A prominent feature is that, upon extending beyond the underneath HMB crystalline substrate, lamellar growth started to develop bending pattern. As further demonstrated in Figure 1b, well-oriented

lamellar growth remains straight, and bending morphology only appears at the ends of loosely oriented edge-on lamellae, i.e., only after losing the contact with underneath substrate is lamellar bending able to develop. In other words, the same mechanism of epitaxial interaction for induced growth of individual edge-on polylactide lamellae into oriented arrays also serves to keep the lamellae from bending. Figure 1a further indicates that lamellar bending on both ends of grown lamellae is mutually correlated, resulting in a Z-shaped or counterclockwise (CCW) bending pattern instead of forming simple scrolls.

It should be noted that, as the crystalline thin film of HMW-PLLA was flipped over when detached from the glass slide, the observed bending sense of arrayed individual PLLA lamellae actually corresponds to an S-shaped or clockwise (CW) pattern if viewed from above the glass slide, in accordance with reported PLLA lamellar growth in ultrathin films as detected via atomic force microscopy.[26] In the following discussion, we will simply follow the TEM-observed sense of lamellar bending to facilitate direct correspondence with the BFI presented herein.

Shown as the inset of Figure 1c, the [100] zone pattern of edge-on lamellae array indicates that the contact plane for epitaxial crystallization corresponds to the *bc* plane of orthorhombic phase.[27] The deviation of *c**-axis from lamellar normal direction (denoted as **n** in the figure) indicates that there is a general CCW tilt of stem packing from lamellar normal by an angle θ ranging from 29° to 42° (with the corresponding lamellar thickness ranging from 9.6 to 12.0 nm), as schematically illustrated in Figure 1d. This observation is novel, as this plane of stem tilt is orthogonal to that conventionally acknowledged at the growth front of flat-on lamellae. More importantly, for studied HMW-PLLA sample, the unique appearance of CCW bending pattern is confirmed to be strictly linked to the presence of CCW deviation of stem orientation. This signifies a direct correlation between the sense of stem tilting from lamellar normal and the sense of lamellar bending developed beyond substrates.

To be consistent with the epitaxial lattice match, the observed stem tilt has to be a result of sequential axial shifting of transverse stems packed within lattice, leading to a stairlike packing scheme on *bc* contact planes as illustrated in Figure 2. The exclusively observed CCW stem tilting indicates that each stem was packed one-step downward relative to its left neighbor on contact plane. Staggered stem packing has been well discussed for the growth of PE single crystals from dilute solutions on the basis of sequential step-descending of stems along both *bc* and *ac* planes in the case of hollow-pyramid crystals with {31*l*} basal planes.[5] A similar mechanism of stem staggering has also been proposed for the α crystal growth of nylon-6,6 as an alternative way to establish hydrogen bonding.[28] The step height in the stairlike stem packing also determines the deviation of lamellar growth from a simple crystallographic direction (such as the *b*-axis in the case of PLLA). According to the variation of measured stem tilt angle θ, this step height is estimated to range from 0.35 to 0.50 nm, which is around the axial length of one repeat unit along the *c*-axis.

Factors Affecting Stem Tilt. For epitaxial crystallization at a lower T_c of 132 °C on the HMB substrate, straight and slightly lamellar bending was frequently found as illustrated in Figure 3a, b. Corresponding SAED patterns indicate that the contact plane is still the *bc* plane for epitaxial crystallization at 132 °C, but the *c**-axis is nearly parallel to the lamellar normal. In other words, at a lower epitaxial crystallization temperature, stem orientation

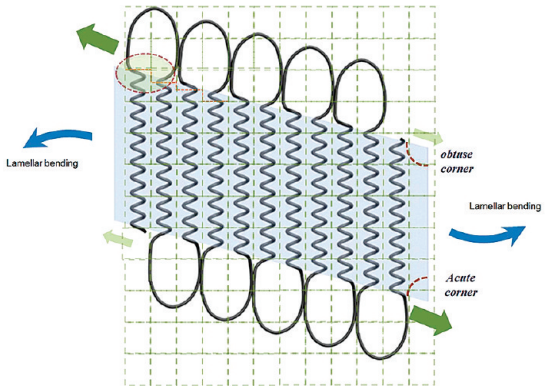

Figure 2. Schematic illustration of stairlike stem packing on contact plane to account for the observed stem tilt, which is manifested with a drawn hypothetic lattice in the background. The downward axial shift, from the left to the right, must prevailingly proceed within edge-on lamellae to result in overall CCW stem tilt. The acute and obtuse corners can be generated due to this stairlike packing. In order to result in CCW bending sense, this drawing manifests that the surface stresses accumulated around the acute corners must be greater than that around obtuse corners. The large green arrows represent the presence of greater surface stresses and vice versa. The red dash circle indicates the step height in the stairlike packing scheme.

only slightly deviates from lamellar normal and epitaxial lamellar growth direction is nearly along the *b*-axis of orthorhombic lattice. Similar trends of chain tilt and nonplanar lamellar growth with increasing growth/annealing temperature have been observed previously.[17,18,29] With the limited extent of stem tilt, an average lamellar thickness was measured to be around 14.0 ± 1.0 nm, greater than that developed at T_c = 150 °C (Figure 3c). For polymer crystal growth, the lamellar thickness is expected to decrease with decreasing T_c; hence, a smaller lamellar thickness for the epitaxial growth at a higher temperature is consistent with the occurrence of stem tilt.

Decreased chain length also results in a lesser extent of stem tilting. Demonstrated in Figure 4b, the orientation of *c**-axis is basically in coincidence with lamellar normal (**n**) according to inset SAED pattern, meaning that stem tilting is barely involved for LMW-PLLA lamellar growth at T_c = 150 °C. The growth direction of edge-on lamellae on substrate surface also parallels the *b*-axis. The measured lamellar thickness is of 14.6 ± 0.9 nm, greater than that of HMW-PLLA lamellae grown at the same T_c of 150 °C. Since at a given crystallization temperature and environment, the transverse stem length is expected to be independent of molecular weight; stem tilting was recognized as a dominant factor to account for the difference in lamellar thickness.

While selected growth temperatures and molecular weights are able to change the extent of stem tilting on *bc* contact plane, the orientation of stem tilting and the bending sense of lamellar growth remain unaffected. Furthermore, as examining the effect from selected chain lengths and growth temperatures, the level of bending tendency appears also linked to the magnitude of stem tilt on contact planes. For evaluating the bending tendency of lamellar growth related to stem tilting, statistic TEM observations are accounted. As lamellar bending beyond underneath substrate is prevailingly observed, a strong bending tendency of extended lamellar growth is considered, and otherwise, a weak bending tendency is classified.

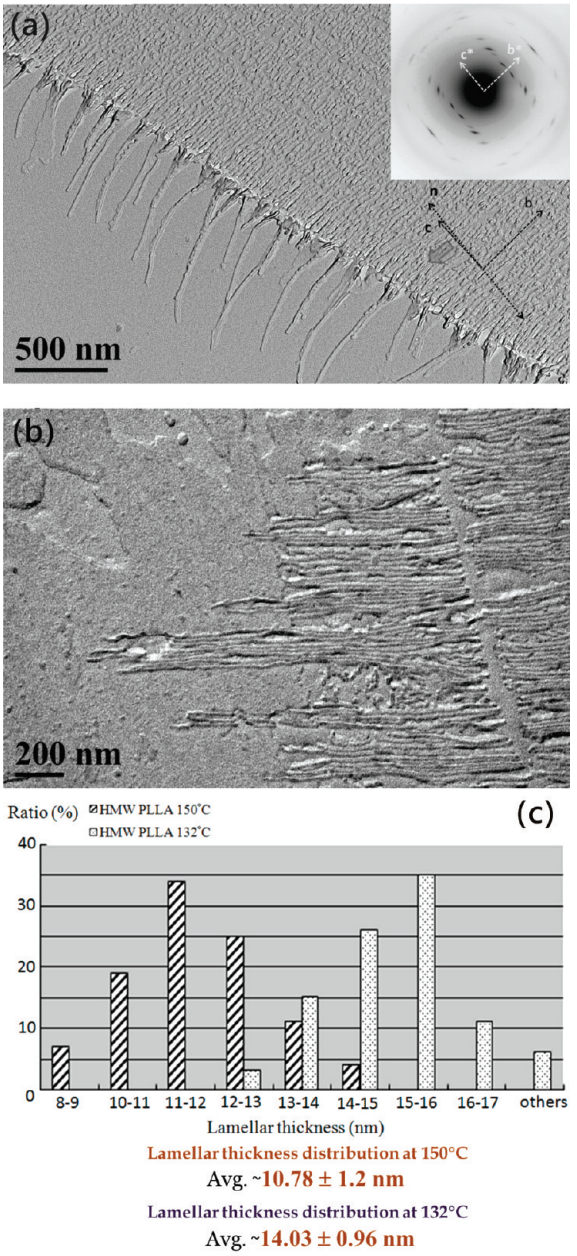

Figure 3. (a) Representative BFI of HMW-PLLA lamellae epitaxially grown at T_c = 132 °C on HMB substrate. The bending tendency appears weaker; only a minor degree of stem tilt is involved as indicated by the inset [100] SAED pattern. (b) Straight lamellar growth beyond the HMB substrate. (c) Effect of growth temperature on lamellar thickness: a lower lamellar growth temperature of 132 °C results in a greater average lamellar thickness as compared with that developed at 150 °C.

Effect of Molecular Chirality. Figure 5 shows arrays of HMW-PDLA edge-on lamellae grown epitaxially on HMB substrate at T_c = 150 °C. The extended growth beyond underneath substrate exhibits modest CW and CCW bending patterns, although the former is observed to occur more frequently; also observed is the presence of straight lamellar growth beyond the substrate (Figure 5b). Hence, we may conclude that a much weaker tendency toward lamellar bending is exhibited by HMW-PDLA. The corresponding SAED indicates that there is merely 6° to 8°of stem tilting relative to

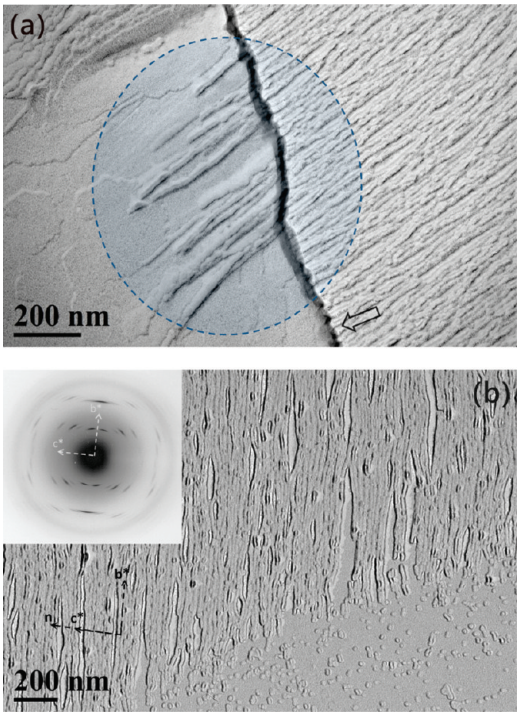

Figure 4. (a) Electron micrograph of LMW-PLLA epitaxial crystallization at T_c = 150 °C on HMB crystalline substrate. The bending tendency appears weaker, and straight lamellar growth beyond substrate is also observed. The substrate edge is indicated by empty arrow. (b) Indicated by the inset [100] SAED pattern; only a minor degree of stem tilt is involved.

lamellar normal, while the *bc* plane of orthorhombic phase still serves as the contact plane. This again agrees with the notion that stem tilting and lamellar bending are closely correlated; nevertheless, in spite of both CW and CCW bending being developed, the stem tilting was recognized to be only CW on the contact plane, which is exactly opposite to that within PLLA edge-on lamellae. This observation suggests some additional contribution of molecular chirality to stem tilting, as we have observed only CW stem tilt within epitaxially grown PDLA lamellae and only CCW stem tilt for PLLA. This specific relationship between molecular chirality and tilting sense of packed stems, not necessary found in other polymeric systems,[30] may probably be related to the difference in the adopted (left- vs right-handed, or 10_7 vs 10_3) helical conformations and should be independent of molecular weight or growth temperature.

DISCUSSION

Stem Axial Shift and Imbalanced Distribution of Surface Stresses. As indicated long ago by Frank,[7] the separation between noncrystalline fold loops on lamellar basal planes is greater than the fixed interstem separations within crystalline planes. Since parts of molecular chain are packed within crystal lattice, the allowed surface areas per connected fold loop on the interphases of lattice packing can be insufficient. This results in crowdedness and mutual repulsions among these noncrystalline molecular segments, which subsequently generates surface stresses on basal planes. To alleviate such crowdedness on basal planes, a feasible way is to organize molecular stems in a staggered manner

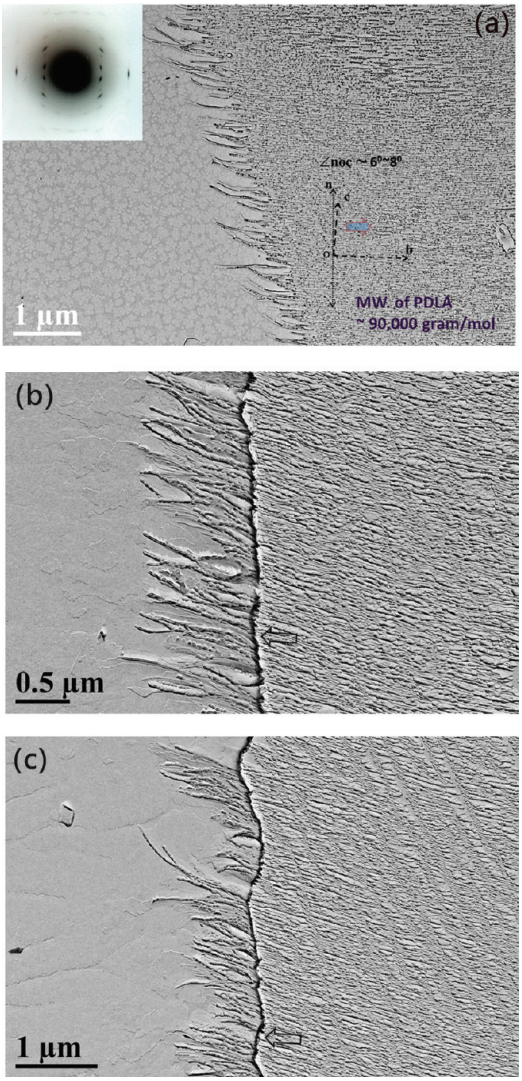

Figure 5. (a) Electron micrograph of HMW-PDLA epitaxial crystallization at T_c = 150 °C on HMB crystalline substrate. Indicated by the inset [100] SAED pattern, only a minor degree of CW (+) stem tilt, about 6° to 8°, is involved. The majority of lamellar bending is CW. (b) Straight lamellar growth beyond the substrate developed frequently. The substrate edge is indicated by empty arrow. (c) Both CW and CCW bending growth can be observed as well. These observations indicate the lack of specific bending sense and weak bending tendency. The substrate edge is indicated by empty arrow.

for gaining larger available surface area per packed stem and per fold loop, as well as reorienting repulsion forces, as illustrated in Figures 2 and 6. This stem stagger via axial shifting of packed stems can regularly take place in a sequential downward or upward manner, which results in stairlike packing. The scheme of stairlike packing accounts for observed deviations of stem orientation from lamellar normal. The step height in stairlike packing can be derived from measured degrees of stem tilt. A larger step height is assumed to reflect a higher level of interface crowdedness. Hence, a greater extent of stem tilt can be linked to larger surface stresses on basal planes, and thus stronger bending tendency.

With recognizing downward sequences of stairlike packing scheme via deviated orientation of stem packing, the locations of

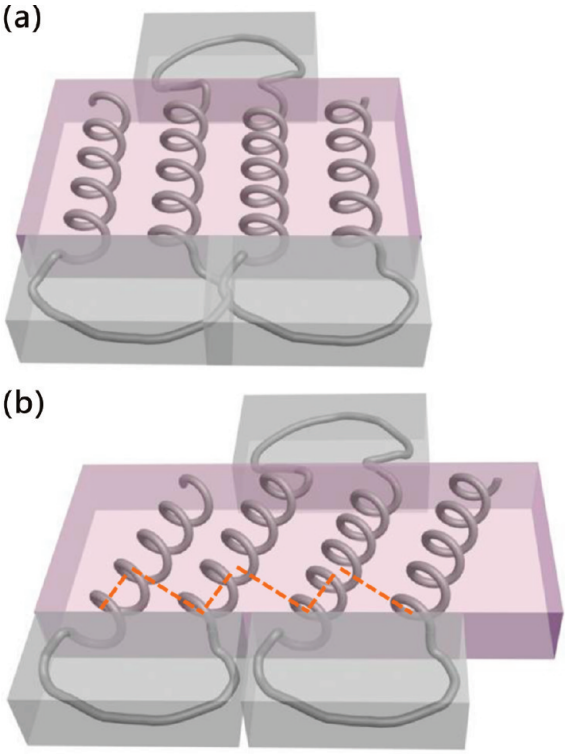

Figure 6. Schematic presentation of stairlike stem packing that results in the observation of stem tilt. Via stem tilt, more space can be created and the repulsion forces can be reoriented. Nevertheless, the loss of lattice interaction on the edge with basal planes is involved, as being emphasized by the red dash line. The gray areas represent schematically the excluded volume of folds.

acute and obtuse corners on growth fronts of each edge-on lamella can be clearly identified as illustrated in Figure 2. (The growth front considered here is for the lamellar growth propagating on substrate surface with the direction indicated in Figure 1d.) The observed overall CCW lamellar bending pattern accordingly acknowledges that larger surface stresses are consistently established around acute corners, whereas around obtuse corners, the present stresses are relatively weaker. Therefore, considering the formation of lamellar corners on opposite growth fronts via stem staggering, this common disparity of stress accumulation does not result in a simple scrolled pattern, but CCW lamellar bending as being illustrated in Figure 1a,b. Since the relative locations of acute and obtuse corners on growth front depend on the orientation of stem tilting, it is understandable to observe a specific relationship between overall lamellar bending patterns, which can be CW or CCW, and stem tilting orientations.

Two dissimilar distribution patterns of fold loops, and thus uneven crowdedness, on each basal plane of selected flat-on lamella have been experimentally identified via surface decoration.[31] This provides molecular interpretations on the cause of lamellar twisting and supports the model of imbalanced accumulation of surface stresses around disparate corners (presumably resulted from differences in dragging molecular stems from approaching molecular coils onto the growth front).[10,11] Nevertheless, the present evidence only provide direct connection between pristine lamellar bending and staggered stem packing on contact plane; a detailed mechanistic evaluation for the origin of uneven

distribution of fold loops on lamellar basal planes awaits further efforts in the future.

Effects from Chain Length and T_c. As well-discussed previously,[3,7] staggered stem packing results in the loss of interstem interactions near the edges of lattice packing located at both the upper and the lower basal planes. Following this concept, the reached extent of stem stagger, indicated by the step height of stairlike packing, only provides compromised reduction of surface crowdedness because further increasing the level of stem staggering is restricted by the loss of lattice energy. The residual surface stress after reaching a certain degree of stem tilt is responsible for observed lamellar bending. Lower mutual repulsion of fold loops represents a lower driving force for stem staggering and, accordingly, only results in a lesser extent of stem tilt.

The degree of stem tilt, reflecting the extent of stem stagger, was found to be influenced by both the molecular weight and growth temperature via altering chain end density and excluded volume on basal planes, as discussed below. Because of a lower molecular weight of LMW-PLLA, the epitaxial growth at 150 °C caused less deviated stem orientation from lamellar normal than that found in the growth of HMW-PLLA lamellae at the same T_c. The measured thickness (14.6 ± 0.9 nm) of LMW-PLLA lamellae corresponds to a twice-folded chain conformation, which results in alternating presence of chain ends and fold loops on basal planes; i.e., the neighbors of a fold loop are expectedly all chain ends. This significantly alleviates interfold repulsion and stress accumulation on basal planes, and therefore a very limited magnitude of stem staggering was experimentally observed for LMW-PLLA lamellae.

With increasing molecular weight, the probability of finding chain ends on lamellar basal planes decreases; surface patterns of fold loops can become less regular also.[18] Hence, the crowdedness on fold surfaces is likely to increase with increasing molecular weight, causing a higher level of stem tilting. Previous studies on the crystallization of PE and paraffins also indicated that the observed lamellar twisting/stem tilting behavior in the crystallization of relatively thick PE films does not occur with paraffins.[32] In addition to molecular weight, with increasing crystallization temperature denoted as T_c, the stem tilt and bending tendency were also found to become more significant. The expansion of fold loop with increasing temperature is presumably responsible for increasing volume exclusion, surface crowdedness, and hence interfold repulsion, subsequently enhancing tendency toward bending. However, various factors can be involved also with the change of growth temperature, like the occurrence of dislocation, and lamellar branching and spray. Some of the factors can possibly decrease the tendency of nonplanar lamellar growth with increasing T_c.[33]

CONCLUSION

Based on the epitaxial relationship established with crystalline surface of HMB nucleation agent, the growth of individual polylactide edge-on lamellae into oriented arrays has been achieved. This experimental design allows lamellar growth free of disturbance from neighbors and results in a simple relationship between lattice packing and lamellar growth habit. After losing contact with underneath substrates, further extended lamellar growth results in concerted lamellar bending instead of simple scrolling. For stem packing on the *bc* contact plane, obtained SAED patterns have indicated orientational deviations from lamellar normal. In view of the presence of lattice match, the observed stem tilting suggests stairlike stem packing on contact planes. The measured magnitude of orientation deviation thus reflects the step height of stairlike packing.

With this stairlike packing of stems, there appear acute and obtuse lamellar corners on growth fronts of each individual lamella. The overall developed lamellar bending pattern indicates greater surface stresses accumulated around acute corners. Since the creation of lamellar corners on growth fronts is related to a regular manner of stem axial staggering, this common disparity of stress accumulation on different type of lamellar corners well accounts for the specific relationship observed between bending senses of lamellar growth and tilting orientation of stem packing; the development of CCW lamellar bending for HMW-PLLA molecules is directly related to CCW deviation of stem packing.

As a consequence of surface overcrowding, the occurrence of stem staggering is expected to alleviate surface stresses, but only to a compromised level in order not to lose excess lattice interaction. This leaves some residual surface stresses responsible for causing the lamellar bending. Effects from molecular weight and growth temperature were discussed in terms of adjustment of chain-end density on lamellar basal planes and the required excluded volume of fold loop, respectively, in relation to changes in surface crowdedness. A greater stem tilting angle (or more severe stem staggering) is assumed to reflect a higher magnitude of crowdedness on basal planes.

For epitaxial lamellar growth of HMW-PDLA on the same crystalline substrate, only an insignificant level of stem tilt is present, and thus developed bending senses are less specific. More importantly, only CW tilt of stem packing has been found, which is opposite to what have been observed in the growth of HMW-PLLA lamellae. This observation signifies that the type of chiral center on polylactide backbone affects the tilted orientation of stem packing developed during lamellar growth, presumably related to adopted helical conformations of different handedness.

ACKNOWLEDGMENT

This work is financially supported by the National Science Council under Grant NSC 98-2221-E-007-009-MY3. Excellent LMW-PLLA and HMW-PDLA samples were kindly provided by Prof. Rong-Ming Ho in Nation Tsing Hua University, and these molecules were synthesized by Ms. Hsin-Wei Wang in Prof. Ho's lab during her study for a master degree. Special thanks are due to the Sustainable Environment Research Center of NCKU for allowing generous accesses to TEM facilities. Helpful discussions with Prof. B. Lotz of Institut Charles Sadron and Prof. G. Strobl of Freiburg University are highly appreciated.

REFERENCES

(1) Blackadder, D. A .; Roberts, T. L. *Makromol. Chem.* **1969**, *126*, 116–129.
(2) Frank, F. C. *Faraday Discuss. Chem. Soc.* **1979**, *68*, 7–13.
(3) Sommer, J.-U. *Lect. Notes Phys.* **2007**, *714*, 19–45.
(4) Basset, D. C.; Hodge, A. M. *Proc. R. Soc. London, Ser. A* **1981**, *377*, 25–37.
(5) Bassett, D. C.; Frank, F. C.; Keller, A. *Nature* **1959**, *184*, 810–811.
(6) Reneker, D. H.; Geil, P. H. *J. Appl. Phys.* **1960**, *31*, 1916–1925.
(7) Bassett, D. C.; Frank, F. C.; Keller, A. *Philos. Mag.* **1963**, *8*, 1739–1751.

(8) Bassett, D. C.; Dammonta, F. R.; Salovey, R. *Polymer* **1964**, *5*, 579–588.
(9) Keller, A. *Kolloid Z. Z. Polym.* **1964**, *197*, 98–115.
(10) Keith, H. D.; Padden, F. J. *Polymer* **1984**, *25*, 28–42.
(11) Keith, H. D.; Padden, F. J. *Macromolecules* **1996**, *29*, 7776–7786.
(12) (a) Lotz, B.; Cheng, S. Z. D. *Polymer* **2005**, *46*, 577–610. (b) Lotz, B.; Cheng, S. Z. D. *Polym. J.* **2008**, *40*, 891–899.
(13) Chao, C.-C.; Chen, C.-K.; Chiang, Y.-W.; Ho, R.-M. *Macromolecules* **2008**, *41*, 3949–3956.
(14) (a) Schultz, J. M.; Kinloch, D. R. *Polymer* **1969**, *10*, 271–278. (b) Yoon, D. Y.; Chang, C.; Stein, R. S. *J. Polym. Sci., Part B: Polym. Phys. Ed.* **1974**, *12*, 2091–2110. (c) Keith, H. D.; Chen, W. Y. *Polymer* **2002**, *43*, 6263–6272.
(15) (a) Toda, A.; Arita, T.; Hikosaka, M. *Polymer* **2001**, *42*, 2223–2233. (b) Abo el Matty, M. I.; Bassett, D. C. *Polymer* **2001**, *42*, 4957–4963. (c) Bassett, D. C. *Philos. Trans. R. Soc. London, A* **1994**, *348*, 29–44. (d) Patel, D.; Bassett, D. C. *Polymer* **2002**, *43*, 3795–3802.
(16) Kumar, S. K.; Yoon, D. Y. *Macromolecules* **1989**, *22*, 3458–3465.
(17) de Silva, D. S. M.; Zeng, X.-B.; Ungar, G.; Spells, S. J. *J. Macromol. Sci., Part B* **2003**, *42*, 915–927.
(18) de Silva, D. S. M.; Zeng, X.-B.; Ungar, G.; Spells, S. J. *Macromolecules* **2002**, *35*, 7730–7741.
(19) Yoon, D. Y.; Flory, P. J. *Macromolecules* **1984**, *17*, 868–871.
(20) (a) Basset, D. C.; Hodge, A. M. *Proc. R. Soc. London, Ser. A* **1978**, *359*, 121–132. (b) Bassett, D. C.; Hodge, A. M.**1981**, *377*, 39–60. (c) Basset, D. C.; Hodge, A. M.**1981**, *377*, 61–71.
(21) (a) Varnell, W. D.; Ryba, E.; Harrison, J. R. *J. Macromol. Sci., Part B: Phys.* **1987**, *26*, 135–143. (b) Voigt-Martin, I. G. *J. Polym. Sci., Polym. Phys.* **1981**, *19*, 1769–1790.
(22) Mandelkern, L. *Acc. Chem. Res.* **1990**, *23*, 380–386.
(23) Gautam, S.; Balijepalli, S.; Rutledge, G. C. *Macromolecules* **2000**, *33*, 9136–9145.
(24) Hocquet, S.; Dosire, M.; Thierry, A.; Lotz, B.; Koch, M. H. J.; Dubreuil, N.; Ivanov, D. A. *Macromolecules* **2003**, *36*, 8376–8384.
(25) Brockway, L. O.; Robertson, J. M. *J. Chem. Soc., Part II* **1939**, 1324–1332.
(26) Maillard, D.; Prud'homme, R. E. *Macromolecules* **2008**, *41*, 1705–1712.
(27) Cartier, L.; Okihara, T.; Ikada, Y.; Tsuji, H.; Puiggali, J.; Lotz, B. *Polymer* **2000**, *41*, 8909–8919.
(28) Wunderlich, B. *Macromolecular Physics*; Academic Press: London, 1973; Vol. I, Chapter 2, p 139.
(29) Xu, J.; Guo, B.-H.; Zhou, J.-J.; Li, L.; Wu, J.; Kowalczuk, M. *Polymer* **2005**, *46*, 9176–9185.
(30) Ye, H.-M.; Xu, J.; Guo, B.-H.; Iwata, T. *Macromolecules* **2009**, *42*, 694–701.
(31) Keith, H. D.; Padden, F. J.; Lotz, B.; Wittmann, J. C. *Macromolecules* **1989**, *22*, 2230–2238.
(32) Wittmann, J. C.; Hodge, A. M.; Lotz, B. *J. Polym. Sci., Part B: Polym. Phys. Ed.* **1983**, *21*, 2495–2509.
(33) Xu, J.; Guo, B.-H.; Zhang, Z.-M.; Zhou, J.-J.; Jiang, Y.; Yan, S.; Li, L.; Wu, Q.; Chen, G.-Q.; Schultz, J. M. *Macromolecules* **2004**, *37*, 4118–4123.